Effect of biodegradation and de novo matrix synthesis on the mechanical properties of VIC-seeded PGS-PCL scaffolds

Shilpa Sant[1,2,3], **Dharini Iyer**[1,2,3], **Akhilesh Gaharwar**[3,4], **Alpesh Patel**[1,2], and **Ali Khademhosseini**[1,2,3,*]

[1]Center for Biomedical Engineering, Department of Medicine, Brigham and Women's Hospital, Harvard Medical School, 65 Landsdowne Street, Cambridge, MA 02139, USA

[2]Harvard-MIT Division of Health Sciences and Technology, Massachusetts Institute of Technology, Cambridge, MA 02139, USA

[3]Wyss Institute for Biologically Inspired Engineering, Harvard University, Boston, MA 02115 USA

[4]David H. Koch Institute for Integrative Cancer Research, Massachusetts Institute of Technology, Cambridge, MA 02139, USA

Abstract

Development of living heart valves that grow with the patient is a promising strategy for heart valve replacements in pediatric patients. Despite the active research in the field of tissue engineered heart valves, there are limited efforts to optimize the balance between biodegradation of the scaffolds and de novo ECM synthesis by the cells and finally, study their consequences on the mechanical properties of the cell-seeded construct. This study investigates the effect of in vitro degradation and extracellular matrix (ECM) secretion on the mechanical properties of hybrid polyester scaffolds. The scaffolds were synthesized from blends of fast degrading polyglycerol sebacate (PGS) and slowly degrading polycaprolactone (PCL). PGS-PCL scaffolds were electrospun using 2:1 ratio of PGS: PCL. Accelerated hydrolytic degradation in 0.1mM sodium hydroxide revealed two fold faster degradation rate for PGS-PCL scaffolds compared to PCL scaffolds. Thermal analysis and scanning electron microscopy demonstrated marginal change in PCL scaffold properties while PGS-PCL scaffolds showed preferential mass loss of PGS and thinning of the individual fibers during degradation. Consequently, mechanical properties of PGS-PCL scaffolds decreased gradually with no significant change for PCL scaffolds during accelerated degradation. Valvular interstitial cells (VICs) seeded on PGS-PCL scaffolds showed higher ECM protein secretion as compared to PCL. Thus, mechanical properties of the cell-seeded PCL scaffolds did not change significantly compared to acellular scaffolds, probably due to slower degradation and ECM deposition by VICs. On the contrary, PGS-PCL scaffolds exhibited gradual decrease in the mechanical properties of the acellular scaffolds due to degradation, which were compensated by new matrix secreted by VICs seeded on the scaffolds. Our study demonstrated that faster degrading PGS component of PGS-PCL accelerated the degradation rate of the

5. Author Contribution

Publisher's Disclaimer: This is a PDF file of an unedited manuscript that has been accepted for publication. As a service to our customers we are providing this early version of the manuscript. The manuscript will undergo copyediting, typesetting, and review of the resulting proof before it is published in its final citable form. Please note that during the production process errors may be discovered which could affect the content, and all legal disclaimers that apply to the journal pertain.

scaffolds. The VICs, on the other hand, were able to remodel the synthetic scaffold, depositing new matrix proteins and maintaining the mechanical properties of the scaffolds.

Keywords

Polyglycerol sebacate; Polycaprolactone; Fibrous scaffolds; Heart valve tissue engineering; In vitro degradation; Mechanical properties; Valve interstitial cells; Extracellular matrix secretion

1. Introduction

Valvular heart disease is a major social and economic burden causing 43,700 deaths in the US in 2006 [1]. Furthermore, Heart valve surgery is the second most common surgery worldwide and is expected to triple over the next thirty years [2]. Although heart valve replacements including mechanical prostheses and bioprostheses have been available clinically, they are non-viable, prone to thromboembolic events and do not grow or remodel after implantation [3]. Thus, pediatric patients will likely need multiple valve replacement operations with age. Tissue engineering offers a great opportunity to build a living heart valve that grows with the patient. Development and optimization of tissue engineered heart valves (TEHV) has been an active area of research over the past few decades. Despite this, the field has been hindered by numerous challenges that include the need for materials that can withstand the demanding biomechanical environment in native valves as well as the ability to guide normal development/repair mechanisms without pathological outcomes such as calcification [4–6].

An understanding of the link between the structure and function of the native valves provides guidance for designing optimum functional TEHV. Native valves open and close approximately 40 million times a year and enable unidirectional blood flow. To achieve the specialized function, valves have a complex and dynamic tissue macro- and microstructure. Trilayered valve architecture consists of specialized extracellular matrix (ECM) composed of collagen, glycosaminoglycans (GAGs) and elastin. Collagen in the fibrosa layer provides tensile strength; central layer of spongiosa rich in GAGs provides necessary hydration and cushioning effect while elastin fibers in ventricularis are necessary for elastic recoil [7, 8]. Ideal scaffold for TEHV should possess mechanical properties to withstand dynamic in vivo environment, should allow cell adhesion, proliferation and ECM secretion by the seeded cells and most importantly, it should degrade at a rate that matches de novo ECM synthesis, thus maintaining the mechanical properties of the constructs [9].

Considering mechanically dynamic environments surrounding heart valves, it is of utmost importance to understand how mechanical properties of TEHV evolve during in vitro culture as well as after subsequent implantation. Engineered cell-seeded scaffolds undergo two important processes, namely, biodegradation and de novo ECM synthesis by the seeded cells. Biodegradation leads to polymer chain scissions and tend to decrease the mechanical properties of the scaffolds whereas new matrix deposition can contribute to the enhanced mechanical properties in the absence of degradation. Hence, an ideal scaffold should possess controlled degradation rate that matches the de novo ECM synthesis and tissue regeneration rate. It is equally essential to understand the relationship between the mechanical properties of the scaffold and the cell-secreted ECM as these two taken together will determine the tissue-level strength of the TEHV and their mechanical performance in vivo [10]. Thus, simultaneous evolution of mechanical properties of the scaffolds as a result of biodegradation and tissue ingrowth should be considered an important step in the fabrication and optimization of TEHV. In this study, we report systematic evaluation of the effect of

degradation and tissue ingrowth on the mechanical properties of VIC seeded tissue engineered constructs.

Various research groups have employed hydrogels as scaffolds for TEHV [11–15]. Although hydrogels provide ECM-mimicking viscoelastic environment and easy functionalization strategies [16–19], their weak initial mechanical and load-bearing properties render them unsuitable for heart valve applications. Synthetic polymers such as polyglycolide, poly-l-lactide, polycaprolactone (PCL) and poly-4-hydroxy butyrate offer tunable mechanical, degradation and processing properties and have shown promising results for fabricating TEHV [20–23]. Due to dynamic and demanding mechanical environments in the native valves, development of elastomeric scaffolds with tunable degradation rate is an attractive strategy for designing flexible TEHV. Polyglycerol sebacate (PGS) is a biodegradable, biocompatible elastomer amenable to various processing techniques like microfabrication [24–26]. It has also shown promising results for soft tissue engineering applications [27–29]. However, PGS has a relatively fast degradation rate that ranges from weeks to months [30–32]. On the other hand, PCL is a semi-crystalline, easy to electrospin polymer having slower rate of degradation [33, 34]. Synthetic polymer blends such as that of PGS and PCL offer advantage of combining properties of different polymers to tune degradation rate, mechanical properties as well as their processability. Recently, we have synthesized fibrous scaffolds using elastomeric PGS and PCL with mechanical properties similar to native human heart valves [35]. The scaffolds also showed enhanced cell adhesion, spreading and proliferation when seeded with human umbilical vein endothelial cells (HUVECs) [35] and human mesenchymal stem cells (hMSCs) [36].

In this work, we have investigated the effect of accelerated in vitro degradation on the physicochemical and mechanical properties of PGS-PCL scaffolds. We have further evaluated the effect of degradation and de novo matrix synthesis by valve interstitial cells (VICs) on the mechanical properties of the scaffolds. We hypothesize that the combination of PGS with PCL will allow controlled degradation of the scaffold. Slowly degrading PCL will provide structural integrity and mechanical support while fast degrading PGS component will create enough space for the new ECM to be deposited, maintaining the mechanical properties of the tissue engineered construct.

2. Materials and Methods

PCL (molecular weight 70–90 kDa), and all other chemicals/solvents were purchased from Sigma-Aldrich (WI, USA). PGS (molecular weight 12 kDa) was synthesized as reported earlier [24]. All cell culture supplies were purchased from Invitrogen (CA, USA).

2.2. Fabrication of fibrous scaffolds

PGS-PCL and PCL scaffolds were fabricated by conventional electrospinning as described earlier [35–37]. Briefly, polymers (33 wt %) were dissolved in a mixture of ethanol and anhydrous chloroform at a volume ratio of 1:9. PGS: PCL weight ratio was kept constant at 2:1. Electrospinning was carried out at 12.5 kV using a 21G blunt needle (Small Parts) and a flow rate of 2 mL/h for ~30 min. The distance between the needle and the collector were kept constant at 18 cm. For easy removal of the fibers, non-adhesive tape was attached to an aluminum plate to collect the fibers. Scaffolds were stored in a desiccator until further use.

2.3. Accelerated In vitro Degradation

2.3.1 Mass loss—Electrospun scaffolds were cut into rectangular strips of 15×5 mm^2 and were subjected to accelerated degradation (n=4) by incubating in 5 ml of 0.1mM sodium hydroxide (NaOH) solution at 37 °C for different time periods. The specimens were

recovered at the end of each degradation time point (1, 3 and 7 days), washed gently with Dulbecco's phosphate buffered saline (DPBS, pH 7.4) and freeze dried. The weight of the degraded sample (W_t) was measured and percentage mass loss the sample was calculated as $((W_o - W_t)/ W_o \times 100)$, based on the initial mass (W_o) of each sample before incubation.

2.3.2 Differential scanning calorimetry (DSC)—Thermal properties of pure polymers and PCL/PGS-PCL scaffolds during degradation were evaluated by differential scanning calorimeter (DSC8500, Perkin-Elmer, USA). The samples were weighed in standard aluminum pans, sealed with lids and heated at the rate of 10 °C/ min from –70 °C to 150 °C and then cooled from 150 °C to –70 °C using nitrogen as a purge gas. Second cycle (heating and cooling) was used to determine melting temperature (T_m), crystallization temperature (T_c) and melting enthalpy (*H*).

2.3.3 Scanning electron microscopy (SEM)—The changes in the microstructure and fiber morphology of the PCL and PGS-PCL scaffolds during degradation were characterized by scanning electron microscope (SEM) (JSM 5600LV, JEOL USA Inc., MA). The electrospun scaffolds were freeze-dried and coated with gold and palladium for 2 min with a Hummer 6.2 sputter coater (Ladd Research, Williston, VT). The images were captured at an acceleration voltage of 5kV and a working distance of 5–10 mm.

2.3.4 Mechanical properties—The effect of accelerated degradation on the mechanical properties of the PCL and PGS-PCL scaffolds was studied by subjecting the degraded scaffolds to uniaxial mechanical testing. The rectangular strips (15×5 mm^2) were subjected to the accelerated degradation as described under section 2.3.1. After each time point, degraded samples (n=4) were removed from NaOH solution, washed gently with PBS and immediately subjected to uniaxial tensile test using eXpert 7601 universal tester (ADMET, Norwood, MA) equipped with 50 N load cell and operated at a crosshead speed of 10 mm/ min. The distance between the grips was set at 5 mm as initial dimension of the test. Elastic moduli (EM) and the ultimate tensile strength (UTS) were determined as the initial slope (5–15% strain) and the highest stress of the stress-strain curve, respectively. Values were reported as mean ± standard deviation (SD).

2.4 Cell viability, proliferation and spreading

2.4.1 Cell culture—Mitral valve interstitial cells (VICs) were provided by Bischoff laboratory at Children's Hospital Boston. Much of the preliminary work relating to the valve cell biology has been conducted in the Bischoff laboratory at Children's Hospital, Boston where the technique of isolating VICs has been optimized, and from these general populations, single cell derived clones have been cultured to obtain homogenous cell populations using the same procedure published previously for aortic and pulmonary valve endothelial cells [38] as well as mitral VICs [39]. VIC clones used in this study were MVICB12 between passage numbers 10–12. The cells were expanded on 1% gelatin-coated dishes in EBM-2 (Endothelial Basal Medium, Lonza) containing 10% heat-inactivated FBS and 1% penicillin/streptomycin.

2.4.2 Cell seeding—Pure PCL and PGS-PCL scaffolds were cut into rectangular strips of dimensions 15×5 mm^2 and sterilized in 70% ethanol for 1h followed by 30 min UV exposure as reported previously [36]. The scaffolds were washed with sterile DPBS prior to seeding. VICs were seeded on each scaffold at a concentration of 200,000 cells/scaffold. The cells were allowed to attach for 12h before transferring them into fresh 24 well plates for longer incubation periods.

2.4.3 Cell viability, proliferation and spreading—To evaluate VIC viability on PCL and PGS-PCL scaffolds, the scaffolds (n=3) were seeded with cells as described above and cultured for 24h and 1 week. The scaffolds were then stained with Live-dead assay kit (Invitrogen), incubated for 20 min at 37 °C and washed with DPBS. Live (green) and dead (red) cells were observed under inverted laser scanning confocal microscope (Leica SP5 X MP) using 10X and 20X objective and images were captured in a sequential imaging mode with z-interval of 0.5 m.

Cell proliferation studies were performed on pure PCL and PGS-PCL scaffolds using the Alamar Blue (AB) assay (Invitrogen). In this assay, viable cells reduce resazurin dye (blue) to resorufin (pink).The reduction of the AB is proportional to the number of viable cells. The VICs were seeded on pure PCL and PGS-PCL scaffolds (n=5) as mentioned above. After 12h, cell-seeded scaffolds were transferred to new 24 well plates and incubated with 500 μL AB solution in EBM2 (10% v/v) for 4h at 37 °C. Blank AB solution served as control. The fluorescence of reduced AB solution (100 μl) was measured using fluorescent plate reader at excitation/ emission wavelength of 550/580 nm.

Cell morphology and cell spreading was assessed by staining the cell seeded scaffolds with actin phallodin (Alexa fluor 594) that specifically stains the actin filaments. VICs on the scaffolds were permeabilized with 0.1% TritonX-100 in PBS (15 min) after fixing with 4% paraformaldehyde (30 min), and stained with actin phalloidin (1:40 in BSA) for 30 min. The nuclei were counterstained using DAPI mounting media (Thermofisher). Images were taken using inverted laser scanning confocal microscope (Leica SP5 X MP) using 20X objective with zoom of 1 and 2 in a sequential imaging mode with z-interval of 0.5 m. Gain, aperture and objectives were kept constant during imaging.

2.5 ECM secretion

To evaluate whether VICs are able to secrete their own ECM, the cells were seeded as described under section 2.4.2 and cultured for 1 and 3 weeks. After the required time interval, the cell-seeded scaffolds (n=3) were fixed with 4% paraformaldehyde and washed with DPBS. The cells were permeabilized with 0.1% Triton X-100 in 1% BSA (15 min). The scaffolds were then incubated with the primary antibodies for 1 h at room temperature (1:200 mouse monoclonal collagen type I (Abcam), 1:200 rabbit monoclonal laminin (Abcam) and 1:200 mouse monoclonal fibronectin (Abcam)). The primary antibodies were prepared in 1% BSA solution. After washing the scaffolds, flurorescein/Alexa Fluor 594 conjugated secondary antibodies (1:200) were added at room temperature (30 min). DAPI solution was used to stain the cell nuclei. The images were taken using laser scanning confocal microscope as described earlier. Gain, aperture and objectives were kept constant during imaging to allow comparison between the samples.

2.6 Mechanical properties

To evaluate the effect of cell seeding and ECM secretion on the mechanical properties of the scaffolds, cells were seeded as described earlier. Scaffolds cultured without cells under similar conditions were used as controls (referred to as 'acellular scaffolds' hereafter). After specified time intervals (1 and 3 weeks), scaffolds without and with cells (n=4) were gently washed with DPBS and subjected to uniaxial tensile testing as described in section 2.3.4.

2.7 Data analysis

All data were expressed as mean ± SD. Student's paired t-test was used for comparisons between two groups. Multiple comparisons were done using one-way/two-way ANOVA followed by Fisher LSD post-hoc test (OriginPro8 SRO, v8.07). *P*-value less than 0.05 were considered significant.

3. Results and Discussion

3.1 Accelerated in vitro degradation

PGS and PCL belong to the class of aliphatic polyesters and degraded by hydrolytic degradation [24, 30, 31, 34]. PCL is a semi-crystalline polymer whereas PGS is amorphous at room temperature. PCL is reported to degrade slowly over a period of 2–4 years depending on its properties such as molecular weight and crystallinity [34] whereas PGS has a faster degradation rate in vivo [30, 32]. To evaluate the degradation properties of PCL and PGS-PCL hybrid scaffolds, we used accelerated conditions using alkaline medium (0.1 mM NaOH) to promote the hydrolysis of polyesters.

3.1.1 Mass loss—As shown in Figure 1A, our results revealed linear degradation profiles for both PCL as well as PGS-PCL scaffolds. PGS-PCL scaffolds showed higher degradation rate (rate constant K= 2.15) as compared to PCL scaffolds (K = 0.82). PCL scaffolds showed only 6% mass loss under accelerated conditions in 7 days as compared to 16% mass loss for PGS-PCL scaffolds. Previous studies on in vivo degradation of PGS implants have shown 70% mass loss linearly in 35 days [30] whereas PCL implants degraded slowly over more than 2 years depending on the molecular weight of PCL [33]. In an accelerated degradation study of PCL scaffolds in higher NaOH concentration (5M), Lam et al also reported mass loss of about 15% in 1 week [34]. However, composite PCL-tri-calcium phosphate scaffolds showed faster rate of degradation due to increased media diffusion. In our previous studies, the addition of PGS led to decreased contact angles of PGS-PCL scaffolds [35]. Hence, it is expected that hydrophilic PGS will enhance the water absorption and thus, rate of degradation of hybrid PGS-PCL scaffolds as compared to PCL scaffolds alone.

3.1.2 Changes in thermal behavior—We further utilized DSC to monitor changes in the thermal behavior of the scaffolds during degradation. DSC thermograms showing heating and cooling cycles of pure PCL polymer and electrospun PCL scaffolds are displayed in Figures 1 B and C, respectively and the results are presented in Table 1. Pure PCL polymer exhibited peak melting temperature (T_m) of 57.8 °C similar to that reported in the literature [40] and melting enthalpy was calculated to be 47.96 J/g. Electrospinning decreased T_m of PCL scaffolds by 1.7 °C, and melting enthalpy (H_{PCL}) was decreased to 26.35 J/g. Such decrease may be attributed to decreased overall crystallinity of PCL during electrospinning as reported previously [40]. However, crystallization temperature (T_c) increased by 3 °C, suggesting decreased chain mobility after electrospinning. Marginal increase (by 1 °C) was also observed in T_m of PCL scaffolds after degradation at day 3 with no further change for day 7. It was also noted that H_{PCL} and T_c did not show any significant change due to degradation.

DSC results for PGS-PCL samples are reported in Figure 1D (heating cycle), 1E (cooling cycle) and Table 2. Pure PGS polymer exhibited two melting endotherms (first sharp and second broad, Fig. 1 D) and T_m of 15 °C (calculated from sharp melting transition) similar to that reported in the literature [41, 42]. Melting enthalpy (H_{PGS}) was found to be 19.13 J/g (Sharp melting curve, Fig. 1D and Table 2). Electrospun PGS-PCL scaffolds also showed two melting endotherms characteristic of PGS (T_m = 12.2°C) and one sharp melting endotherm for PCL (T_m = 55.8 °C). The corresponding values for PGS and PCL were 2–3 °C lower than the T_m corresponding pure polymers, suggesting decreased overall crystallinity due to the electrospinning process and/or presence of other polymer [40]. Degradation did not show any change in T_m of PGS whereas that of PCL showed marginal increase similar to pure PCL scaffolds (Table 1). H_{PCL} and H_{PGS} decreased by 2 J/g after 3 days degradation, showing no change thereafter (Table 2). It is possible that PGS on the

surface of PGS-PCL scaffolds was degraded and leached out within 3 days; however, PGS that was surrounded by PCL during electrospinning was possibly not accessible for hydrolysis until outer slowly degrading PCL is hydrolyzed. This may have resulted in minor or no changes in the thermal properties after day 3. However, both melting and crystallization peaks of PGS disappeared gradually suggesting loss of PGS from PGS-PCL scaffolds during degradation (Fig. 1D and inset in 1E). Although pure PGS polymer exhibited single peak with a shoulder, PGS-PCL scaffolds exhibited multiple peaks during crystallization (Inset, Fig. 1E). It is also noted that PCL exhibited subsequent increase in the crystallization peak. This phenomenon may be attributed to the preferential degradation of amorphous zones, especially PGS, increasing crystallization ability of PCL [43]. Thus, thermal property changes further supported mass loss data in Figure 1A suggesting faster degradation of PGS-PCL scaffolds compared to PCL scaffolds.

3.1.3 Morphological changes—The DSC results of in vitro degradation were further confirmed by morphological characterization using SEM. As shown in Figure 2, PCL scaffolds did not show any microscopic changes in fiber morphology during accelerated degradation in 0.1 mM NaOH over the period of 7 days. On the other hand, PGS-PCL fibers displayed porous structure formation on day 7 as evident from SEM images (Fig. 2, indicated by white arrowheads). Previous studies have reported that PGS degrades preferentially by surface erosion mechanism [30, 31]. Our study also suggested surface erosion dominated degradation of PGS-PCL scaffolds as evident by linear mass loss (Fig. 1A) and SEM images (Fig. 2).

3.1.4 Mechanical properties—Ideally, biodegradable scaffolds designed for tissue engineering applications should provide necessary structural integrity and mechanical support to the seeded cells. Initial mechanical properties of the scaffolds should match those of the regenerating tissues, in this case, heart valves. PGS-PCL hybrid scaffolds have shown mechanical properties similar to the native human valve leaflets [35, 44]. However, degradation affects the structural integrity and mechanical properties. Hence, for optimum scaffold performance, it is important to study the changes in the mechanical properties during degradation.

Mechanical properties of both PCL and PGS-PCL scaffolds during accelerated in vitro degradation are shown in Figure 3. Consistent with the mass loss, DSC and SEM results, there were no significant changes in the elastic modulus (stiffness, EM) and ultimate tensile stress (UTS) of PCL scaffolds. UTS of PCL scaffolds reduced from 3.38±0.5 to 2.88±0.17 MPa after 7 days accelerated degradation. EM also showed insignificant change from 7.4±0.62 to 7.0±0.13 MPa after 7 days. On the other hand, UTS and EM values decreased slowly and significantly for PGS-PCL scaffolds after days 3 and 7 during degradation (p < 0.05, one way ANOVA). For instance, UTS decreased from 3.5±0.5 to 1.95±0.17 MPa on day 7 while EM values dropped from 7.8±0.45 to 4.5±0.3 MPa after 7 days of accelerated degradation. The significant reduction in the mechanical properties of PGS-PCL scaffolds can be correlated to the higher mass loss shown in Figure 1A. It is reported that the process of degradation leads to hydrolytic polymer chain scissions, thus creating weak points/defects in the structure and reducing the mechanical properties of the scaffolds over period of time [34]. Similar behavior has been reported for other polymeric scaffolds and composites such as PLGA [45], poly (1,8 octanediol-co-citrate) [46] and polyester-urethanes [47].

3.2 VIC viability, proliferation and spreading

Heart valves contain two major cell populations, namely, valvular interstitial cells (VICs) and valvular endothelial cells. VICs play an important role in extracellular matrix (ECM) synthesis and remodeling. Valvular ECM, in turn, regulates the VIC function and phenotype

and thus, maintains mechanical and physical properties of the valves [8]. It is also suggested that ECM quality depends on VIC viability and function. Non-viable VICs, altered collagen and other ECM molecules often lead to pathologic outcomes such as calcification of bioprosthetic valves [48]. Thus, it is important that the engineered scaffolds support viability and growth of VICs. To test this, VICs were seeded on the sterilized PCL and PGS-PCL scaffolds and were evaluated for their viability, proliferation and spreading.

Figure 4 A shows maximum projection of representative confocal Z-stacks of VICs seeded on electrospun scaffolds. The cells were able to maintain their viability (cells stained green) on both scaffolds. The cells were able to proliferate as evidenced by increased number of fluorescent cells over a period of 7 days. The metabolic activity assay using alamar blue also revealed increased metabolic activity of VICs seeded on both PCL and PGS-PCL scaffolds. Figure 5 shows confocal images of VICs stained for actin filaments after 1 and 7 days in culture. It was observed that the VICs exhibited rounded morphology on PCL scaffolds while PGS-PCL scaffolds promoted cell spreading as early as day 1. However, all the cells showed spread morphology by day 7. The ability of both scaffolds to promote proliferation was also confirmed by actin staining evidenced by increased number of cells after 7 day culture. As per our previous studies, PGS-PCL scaffolds supported cell viability, attachment, proliferation and spreading for various types of cells including HUVECs [35] and hMSCs [36]. According to our previous data, the addition of PGS decreases the contact angle and hydrophobicity of PCL, leading to enhanced cell attachment and spreading [35].

3.3 ECM secretion and mechanical properties of VIC-seeded scaffolds

For successful heart valve tissue engineering, in addition to the suitable degradation rate and biocompatibility, scaffolds should also promote the ability of the VICs to remodel and regenerate the tissue by secreting their own ECM, eventually, replacing the synthetic scaffold material completely [8]. Thus, tissue regeneration using biodegradable scaffolds and cells involves degradation of the scaffolds and tissue ingrowth concurrently and both these processes lead to evolution of the structural and mechanical properties of the engineered tissue construct. As discussed earlier, biodegradation leads to defects in the polymer backbone, thereby compromising structural integrity and reducing mechanical properties. On the other hand, it is expected that mechanical properties of the tissue engineered construct will increase as the cells grow and remodel the synthetic matrix by laying down new matrix. Thus, optimal design of scaffolds for tissue regeneration should evaluate simultaneous effect of biodegradation and tissue ingrowth on their mechanical properties.

VICs have the ability to secrete various proteins such as collagen (Type I, III and IV), laminin and fibronectin [49]. Collagen is a major component of ECM in heart valves and provides mechanical strength and maintains tissue integrity [8]. Basement membrane proteins such as laminin play an important role in multiple cell signaling pathways and are secreted by VICs [49]. Similarly, fibronectin, an adhesive glycoprotein plays an important role in wound healing and repair and is secreted by migrating VICs during valve repair [50]. Based on these reports from the literature, we investigated the ability of VICs seeded on fibrous PCL and PGS-PCL scaffolds to secrete fibrous proteins, specifically, Collagen Type I (COL I), Laminin (LN) and Fibronectin (FN). Elastin is another major ECM component providing necessary elastic properties to the native heart valves. However, VICs themselves cannot synthesize elastin fibers in 2D culture [49]. Elastin formation has been recognized as a missing link in tissue engineered tissue constructs [51]. Nonetheless, we evaluated elastin secretion by VICs on both PCL and PGS-PCL fibrous scaffolds. However, we could not find any elastin secretion by VICs in our study. We also compared the effect of ECM secretion and scaffold degradation on the mechanical properties of VIC seeded scaffolds with their acellular counterparts cultured in the VIC media.

3.3.1 PCL scaffolds—The ability of VICs to secrete COL I, FN and LN when seeded on PCL scaffolds was investigated after 1 and 3 weeks in culture. Secreted ECM proteins were stained using respective antibodies as described under section 2.5 and z-stacks of immunofluorescence images were captured by confocal laser scanning microscope. As shown in Figure 6A, VICs were able to secrete COL-I, FN and LN on PCL scaffolds. Expression of COL I and LN were found to be mainly intracellular over the period of culture time while FN networks were secreted extracellularly around the cells. Flanagan et al have reported similar expression pattern for the ECM proteins in two-dimensional VIC cultures in their study [49]. COL I production did not seem to increase in time-dependent manner when compared between 1 and 3 weeks. Higher LN production was observed after 3 weeks; however, time-dependent increase in secretion was more prominent for FN. It is worthwhile to note the increased number of nuclei from 1 week to 3 week further supporting viability and growth of VICs on these scaffolds.

Mechanical properties were evaluated for cell seeded scaffolds and compared with acellular PCL scaffolds cultured under the same conditions. Acellular PCL scaffolds (D0, Fig. 6 B) showed UTS of 3.38 ± 0.53 MPa which was changed marginally to 3.18 ± 0.8 MPa over a period of 3 weeks. VIC-seeded PCL scaffolds showed increasing trend in UTS over 3 weeks period. For instance, UTS of cell-seeded scaffolds increased to 3.75 ± 0.42 MPa (Fig. 6 B). Overall, two-way ANOVA revealed that time and cell seeding had no significant effect on the UTS of PCL scaffolds ($P > 0.05$). EM of acellular scaffolds decreased from initial value of 7.48 ± 0.62 MPa to 5.73 ± 0.33 MPa after 3 weeks degradation (Fig. 6 C). Although no significant decrease was observed until 2 weeks, EM of acellular scaffolds decreased significantly after 3 weeks degradation. This suggested that PCL scaffolds may have started degradation process sufficient to affect just the stiffness but not the tensile strength of the scaffolds. Cell-seeded PCL scaffolds showed higher values of EM compared to acellular scaffolds at the same time. However, statistically significant increase was observed only at week 3. EM of cell-seeded scaffolds increased to 7.9 ± 0.48 MPa which was statistically higher than acellular scaffolds (5.73 ± 0.33 MPa). Overall, two way ANOVA revealed that both time and cell seeding affected EM of PCL scaffolds. Such statistically significant changes were evident only at longer time of 3 weeks, may be due to sufficient time allowed for scaffold degradation as well as ECM secretion, both processes contributing to the opposite effects on the final stiffness of the constructs. However, it is noteworthy that of cell-seeded scaffolds at 3 week showed comparable EM values to that of as-fabricated PCL scaffolds, thus compensating for the decrease in EM due to degradation at same time.

3.3.2 PGS-PCL scaffolds—VICs seeded on the PGS-PCL scaffolds produced much higher amount of COL I, FN and LN than PCL scaffolds as shown by higher ECM staining for these proteins in Figure 7A. Time-dependent increase in the COL I and LN expression was also evident after 3 weeks as compared to 1 week. Although LN expression appeared to be more restricted intracellularly, FN networks were found to be extracellular similar to that observed in PCL scaffolds in other study [49]. COL I staining appeared to be intracellular for 1 week group; however, dense collagen network was formed after 3 weeks.

Acellular and cell-seeded PGS-PCL scaffolds showed more prominent differences in mechanical properties compared to PCL scaffolds. Representative stress-strain curves for acellular PGS-PCL scaffolds (Day 0, week 1 and week 3) and cell-seeded scaffolds (week 1 and week 3) have been presented as supplementary figure for comparison of changes in the mechanical properties over time. UTS of acellular PGS-PCL scaffolds decreased gradually over a period of 3 weeks as shown in Figure 7B and consistent with accelerated in vitro degradation (Fig. 3). UTS of as-fabricated PGS-PCL scaffolds (D0 in Fig. 7B) was 3.48 ± 0.5 MPa and was decreased to 2.4 ± 0.32 MPa after immersion in culture medium for 3 weeks. Similarly, EM of acellular PGS-PCL scaffolds decreased two folds from 7.8 ± 0.45 MPa at

day 0 to 3.63±0.79 MPa after 3 weeks in culture. It is noteworthy that VIC-seeded PGS-PCL scaffolds were able to maintain the mechanical properties of the scaffolds compared to day 0 as shown in Figure 7A. This effect was evident at longer time point of 3 weeks. For instance, cell seeding increased UTS to 3.53±0.19 MPa compared to 2.4±0.32 MPa for acellular scaffolds after weeks culture time. Similarly, cell-seeded scaffolds showed significantly higher EM (9.28±0.43 MPa) after 3 weeks VIC culture compared to scaffolds without cells (3.63±0.79 MPa) cultured under the same conditions. This may be attributed to the deposition of cell-secreted ECM molecules as shown in Figure 7A. Similar increase in the stiffness of cell-seeded scaffolds due to new ECM deposition has been reported recently in cartilage tissue engineering [52]. It is also possible that the presence of cells themselves and/or cell-secreted matrix reduced the degradation rate of the underlying polymer scaffolds, consequently maintaining/increasing the overall mechanical properties of the VIC-seeded scaffolds.

Although elastin is another most important ECM component of native heart valves, culture of VICs on PGS-PCL scaffolds could not promote elastin synthesis. Currently, we are developing strategies to overcome the major limitation of our study. Another important aspect that remains to be addressed here is the anisotropic structure of heat valve tissue with distinct collagen fiber orientation and mechanical properties in the circumferential and radial directions [7]. The suitability of PGS-PCL scaffolds to recreate this anisotropy and its potential for heart valve tissue engineering will be investigated in the future studies.

Conclusion

We investigated the effect of accelerated in vitro degradation on the thermal behavior, microstructure as well as mechanical properties of PGS-PCL scaffolds. Mass loss, DSC and SEM results confirmed faster degradation of PGS-PCL scaffolds with preferential mass loss of PGS polymer. PGS-PCL scaffolds also exhibited gradual changes in the mechanical properties during accelerated degradation as well as physiological conditions using culture medium. VICs showed good viability, metabolic activity and spread morphology on both PCL and PGS-PCL scaffolds. VICs deposited higher amount of ECM proteins on PGS-PCL scaffolds compared to PCL scaffolds. Thus, VICs were able to remodel synthetic PGS-PCL scaffolds and balance the mechanical properties due to biodegradation and tissue ingrowth, suggesting potential application of PGS-PCL scaffolds for heart valve tissue engineering.

Supplementary Material

Refer to Web version on PubMed Central for supplementary material.

Acknowledgments

References

1. Roger VL, Go AS, Lloyd-Jones DM, Benjamin EJ, Berry JD, Borden WB, et al. Heart disease and stroke statistics - 2012 update. A report from the American Heart Association. Circulation. 2012; 125(1):E2–E220. [PubMed: 22179539]

2. Yacoub MH, Takkenberg JJM. Will heart valve tissue engineering change the world? Nat Clin Pract Cardiovasc Med. 2005; 2(2):60–1. [PubMed: 16265355]

3. Butcher JT, Mahler GJ, Hockaday LA. Aortic valve disease and treatment: the need for naturally engineered solutions. Adv Drug Deliv Rev. 2011 Apr 30; 63(4–5):242–268. [PubMed: 21281685]

4. Mol A, Smits AIPM, Bouten CVC, Baaijens FPT. Tissue engineering of heart valves: advances and current challenges. Expert Rev Med Devices. 2009 May; 6(3):259–275. [PubMed: 19419284]

5. Schoen FJ. Heart valve tissue engineering: quo vadis? Curr Opin Biotech. 2011; 22(5):698–705. [PubMed: 21315575]

6. Sewell-Loftin MK, Chun YW, Khademhosseini A, Merryman WD. EMT-inducing Biomaterials for heart valve Engineering: Taking Cues from Developmental Biology. J Cardiovasc Trans Res. 2011 Oct; 4(5):658–671.

7. Sacks MS, Yoganathan AP. Heart valve function: a biomechanical perspective. Philos Trans R Soc B Biol Sci. 2007 Aug; 362(1484):1369–1391.

8. Schoen FJ. Evolving Concepts of Cardiac Valve Dynamics The continuum of Development, Functional Structure, Pathobiology, and Tissue Engineering. Circulation. 2008; 118(18):1864–1880. [PubMed: 18955677]

9. Brody S, Pandit A. Approaches to heart valve tissue engineering scaffold design. J Biomed Mater ResPart B. 2007 Oct; 83B(1):16–43.

10. Engelmayr GC Jr, Sacks MS. Prediction of extracellular matrix stiffness in engineered heart valve tissues based on nonwoven scaffolds. Biomech Model Mechanobiol. 2008 Aug; 7(4):309–321. [PubMed: 17713801]

11. Shah DN, Recktenwall-Work SM, Anseth KS. The effect of bioactive hydrogels on the secretion of extracellular matrix molecules by valvular interstitial cells. Biomaterials. 2008; 29(13):2060–2072. [PubMed: 18237775]

12. Gupta V, Werdenberg JA, Blevins TL, Grande-Allen KJ. Synthesis of glycosaminoglycans in differently loaded regions of collagen gels seeded with valvular interstitial cells. Tissue Eng. 2007; 13(1):41–49. [PubMed: 17518580]

13. Flanagan TC, Wilkins B, Black A, Jockenhoevel S, Smith TJ, Pandit AS. A collagen-glycosaminoglycan co-culture model for heart valve tissue engineering applications. Biomaterials. 2006 Apr; 27(10):2233–2246. [PubMed: 16313955]

14. Robinson PS, Johnson SL, Evans MC, Barocas VH, Tranquillo RT. Functional Tissue-Engineered Valves from Cell-Remodeled Fibrin with Commissural Alignment of Cell-Produced Collagen. Tissue Eng A. 2008; 14(1):83–95.

15. Benton JA, DeForest CA, Vivekanandan V, Anseth KS. Photocrosslinking of Gelatin Macromers to Synthesize Porous Hydrogels That Promote Valvular Interstitial Cell Function. Tissue Eng Part A. 2009; 15(11):3221–3230. 2009/11/01. [PubMed: 19374488]

16. Jia XQ, Kiick KL. Hybrid Multicomponent Hydrogels for Tissue Engineering. Macromol Biosci. 2009 Feb; 9(2):140–156. [PubMed: 19107720]

17. Slaughter BV, Khurshid SS, Fisher OZ, Khademhosseini A, Peppas NA. Hydrogels in Regenerative Medicine. Adv Mater. 2009 Sep; 21(32–33):3307–3329. [PubMed: 20882499]

18. Yamanlar S, Sant S, Boudou T, Picart C, Khademhosseini A. Surface functionalization of hyaluronic acid hydrogels by polyelectrolyte multilayer films. Biomaterials. 2011; 32(24):5590–5599. [PubMed: 21571364]

19. Sant S, Hancock MJ, Donnelly JP, Iyer D, Khademhosseini A. Biomimetic gradient hydrogels for tissue engineering. Can J Chem Eng. 2010; 88(6):899–911. [PubMed: 21874065]

20. Sodian R, Hoerstrup SP, Sperling JS, Daebritz S, Martin DP, Moran AM, et al. Early in vivo experience with tissue-engineered trileaflet heart valves. Circulation. 2000 Nov 7; 102(19):22–29.

21. Del Gaudio C, Grigioni M, Bianco A, De Angelis G. Electrospun bioresorbable heart valve scaffold for tissue engineering. Int J Artif Organs. 2008 Jan; 31(1):68–75. [PubMed: 18286457]

22. Schaefermeier PK, Szymanski D, Weiss F, Fu P, Lueth T, Schmitz C, et al. Design and Fabrication of Three-Dimensional Scaffolds for Tissue Engineering of Human Heart Valves. Eur Surg Res. 2009; 42(1):49–53. [PubMed: 18987474]

23. Ramaswamy S, Gottlieb D, Engelmayr GC Jr, Aikawa E, Schmidt DE, Gaitan-Leon DM, et al. The role of organ level conditioning on the promotion of engineered heart valve tissue development in-vitro using mesenchymal stem cells. Biomaterials. 2010; 31(6):1114–1125. [PubMed: 19944458]

24. Wang YD, Ameer GA, Sheppard BJ, Langer R. A tough biodegradable elastomer. Nat Biotechnol. 2002 Jun; 20(6):602–606. [PubMed: 12042865]

25. Ifkovits JL, Devlin JJ, Eng G, Martens TP, Vunjak-Novakovic G, Burdick JA. Biodegradable Fibrous Scaffolds with Tunable Properties formed from Photo-Cross-Linkable Poly(glycerol sebacate). ACS Appl Mater Interface. 2009; 1(9):1878–1886.

26. Bettinger CJ, Orrick B, Misra A, Langer R, Borenstein JT. Micro fabrication of poly(glycerol-sebacate) for contact guidance applications. Biomaterials. 2006 Apr; 27(12):2558–2565. [PubMed: 16386300]

27. Fidkowski C, Kaazempur-Mofrad MR, Borenstein J, Vacanti JP, Langer R, Wang YD. Endothelialized microvasculature based on a biodegradable elastomer. Tissue Eng. 2005; 11(1–2): 302–309. [PubMed: 15738683]

28. Engelmayr GC, Cheng MY, Bettinger CJ, Borenstein JT, Langer R, Freed LE. Accordion-like honeycombs for tissue engineering of cardiac anisotropy. Nat Mater. 2008 Dec; 7(12):1003–1010. [PubMed: 18978786]

29. Lee K-W, Stolz DB, Wang Y. Substantial expression of mature elastin in arterial constructs. P Natl Acad Sci USA 2011. Jan 31.2011

30. Wang YD, Kim YM, Langer R. In vivo degradation characteristics of poly(glycerol sebacate). J Biomed Mater Res Part A. 2003 Jul; 66A(1):192–197.

31. Pomerantseva I, Krebs N, Hart A, Neville CM, Huang AY, Sundback CA. Degradation behavior of poly(glycerol sebacate). J Biomed Mater Res Part A. 2009 Dec 15; 91A(4):1038–1047.

32. Sundback CA, Shyu JY, Wang YD, Faquin WC, Langer RS, Vacanti JP, et al. Biocompatibility analysis of poly(glycerol sebacate) as a nerve guide material. Biomaterials. 2005 Sep; 26(27): 5454–5464. [PubMed: 15860202]

33. Sun H, Mei L, Song C, Cui X, Wang P. The in vivo degradation, absorption and excretion of PCL-based implant. Biomaterials. 2006; 27(9):1735–1740. [PubMed: 16198413]

34. Lam CXF, Savalani MM, Teoh S-H, Hutmacher DW. Dynamics of in vitro polymer degradation of polycaprolactone-based scaffolds: accelerated versus simulated physiological conditions. Biomed Mater. 2008; 3(3):034108. [PubMed: 18689929]

35. Sant S, Hwang CM, Lee S-H, Khademhosseini A. Hybrid PGS–PCL microfibrous scaffolds with improved mechanical and biological properties. J Tissue Eng Regen Med. 2011; 5(4):283–291. [PubMed: 20669260]

36. Tong Z, Sant S, Khademhosseini A, Jia X. Controlling the Fibroblastic Differentiation of Mesenchymal Stem Cells Via the Combination of Fibrous Scaffolds and Connective Tissue Growth Factor. Tissue Eng A. 2011 Jan 11; 17A(21–22):2773–2785.

37. Sant S, Khademhosseini A. Fabrication and characterization of tough elastomeric fibrous scaffolds for tissue engineering applications. Conf Proc IEEE Eng Med Biol Soc. 2010; 1:3546–3548. [PubMed: 21096824]

38. Paranya G, Vineberg S, Dvorin E, Kaushal S, Roth SJ, Rabkin E, et al. Aortic Valve Endothelial Cells Undergo Transforming Growth Factor-β-Mediated and Non-Transforming Growth Factor-β-Mediated Transdifferentiation in Vitro. Am J Pathol. 2001; 159(4):1335–1343. [PubMed: 11583961]

39. Wylie-Sears J, Aikawa E, Levine RA, Yang J-H, Bischoff J. Mitral Valve Endothelial Cells With Osteogenic Differentiation Potential. Arterioscler Thromb Vasc Biol. 2011 Mar; 31(3):598–U266. [PubMed: 21164078]

40. Bolgen N, Menceloglu YZ, Acatay K, Vargel I, Piskin E. In vitro and in vivo degradation of non-woven materials made of poly(epsilon-caprolactone) nanofibers prepared by electrospinning under different conditions. J Biomater Sci Polym Ed. 2005; 16(12):1537–1555. [PubMed: 16366336]

41. Cai W, Liu L. Shape-memory effect of poly(glycerol-sebacate) elastomer. Mater Lett. 2008; 62(14):2171–2173.

42. Liu QY, Tian M, Shi R, Zhang LQ, Chen DF, Tian W. Structure and properties of thermoplastic poly(glycerol sebacate) elastomers originating from prepolymers with different molecular weights. J Appl Polym Sci. 2007 Apr; 104(2):1131–1137.

43. Hua J, Gebarowska K, Dobrzynski P, Kasperczyk J, Wei J, Li S. Influence of Chain Microstructure on the Hydrolytic Degradation of Copolymers from 1,3-Trimethylene Carbonate and L-Lactide. J Polym Sci Pol Chem. 2009 Aug 1; 47(15):3869–3879.

44. Balguid A, Rubbens MP, Mol A, Bank RA, Bogers A, Van Kats JP, et al. The role of collagen cross-links in biomechanical behavior of human aortic heart valve leaflets - Relevance for tissue engineering. Tissue Eng. 2007 Jul; 13(7):1501–1511. [PubMed: 17518750]

45. Perron JK, Naguib HE, Daka J, Chawla A, Wilkins R. A study on the effect of degradation media on the physical and mechanical properties of porous PLGA 85/15 scaffolds. J Biomed Mater Res Part B. 2009; 91B(2):876–886.

46. Jeong CG, Hollister SJ. Mechanical, permeability, and degradation properties of 3D designed poly(1,8 octanediol-co-citrate) scaffolds for soft tissue engineering. J Biomed Mater Res Part B. 2010; 93B(1):141–149.

47. Krynauw H, Bruchmüller L, Bezuidenhout D, Zilla P, Franz T. Degradation-induced changes of mechanical properties of an electro-spun polyester-urethane scaffold for soft tissue regeneration. J Biomed Mater Res Part B. 2011; 99B(2):359–368.

48. Schoen FJ, Levy RJ. Calcification of Tissue Heart Valve Substitutes: Progress Toward Understanding and Prevention. Ann Thorac Surg. 2005; 79(3):1072–1080. [PubMed: 15734452]

49. Flanagan TC, Black A, O'Brien M, Smith TJ, Pandit AS. Reference models for mitral valve tissue engineering based on valve cell phenotype and extracellular matrix analysis. Cells Tissues Organs. 2006; 183(1):12–23. [PubMed: 16974091]

50. Fayet C, Bendeck MP, Gotlieb AI. Cardiac valve interstitial cells secrete fibronectin and form fibrillar adhesions in response to injury. Cardiovasc Pathol. 2007; 16(4):203–211. [PubMed: 17637428]

51. Patel A, Fine B, Sandig M, Mequanint K. Elastin biosynthesis: the missing link in tissue-engineered blood vessels. Cardiovasc Res. 2006 Jul 1; 71(1):40–49. [PubMed: 16566911]

52. Huang AH, Yeger-McKeever M, Stein A, Mauck RL. Tensile properties of engineered cartilage formed from chondrocyte- and MSC-laden hydrogels. Osteoarthritis Cartilage. 2008 Sep; 16(9):1074–1082. [PubMed: 18353693]
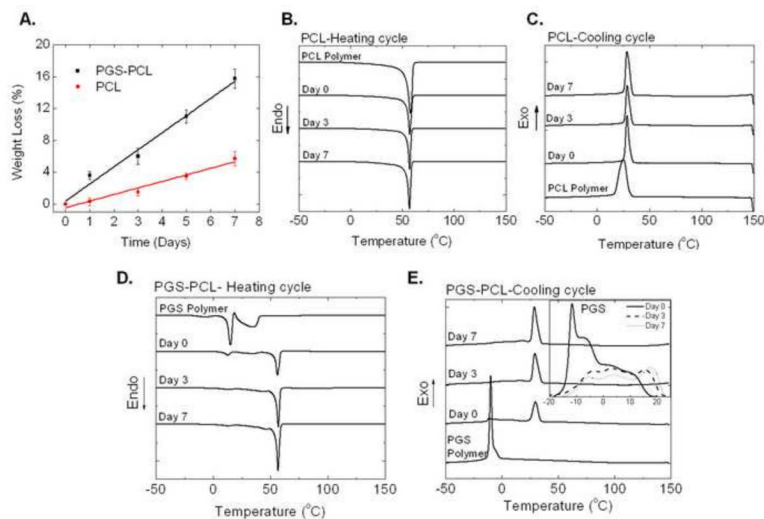
Fig. 1.
Accelerated in vitro degradation of PCL and PGS-PCL in 0.1mM NaOH. A. Weight loss (%); Differential scanning calorimetric (DSC) curves showing B. melting transition (second heating cycle) and C. crystallization transition (cooling cycle) of PCL; D. melting transition (second heating cycle) and E. crystallization transition (cooling cycle) of PGS-PCL scaffolds during degradation. Inset in (E) shows changes in PGS crystallization peaks during degradation. PGS-PCL scaffolds showed faster degradation as revealed by weight loss data as well as DSC data. PCL did not show significant thermal changes. On the other hand, both heating as well as cooling cycles of PGS-PCL showed disappearance of PGS peaks as well as increase in the crystallization enthalpy of PCL in PGS-PCL scaffolds, suggesting changes in the polymer composition during degradation.
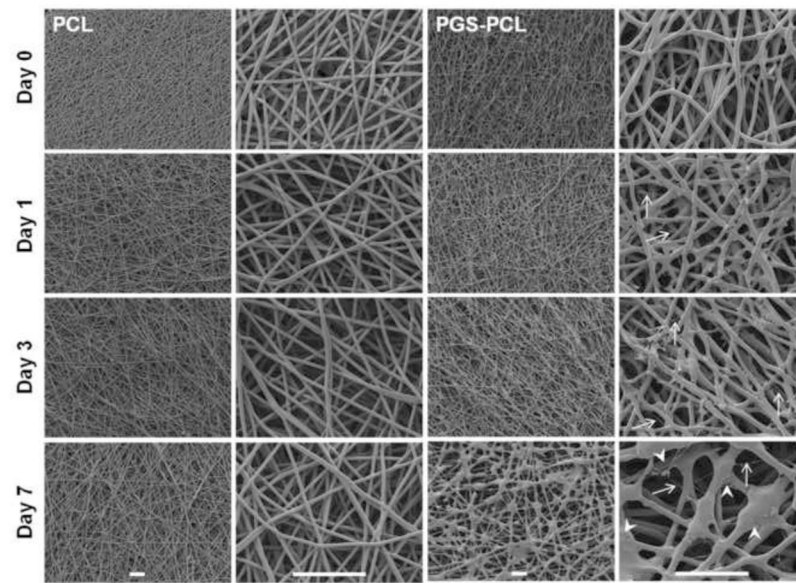
Fig. 2.
Scanning electron microscopy images of PCL and PGS-PCL scaffolds during accelerated degradation studies.PCL fibers did not show any morphological changes over the period of 7 days whereas PGS-PCL fibers showed significant morphological changes including swelling and fiber degradation as indicated by presence of thinner fibers (white arrows). In addition, multiple porous structures were present on the underlying fiber layers indicating onset of degradation of these fibers (white arrowheads). Morphological changes were seen only in the uppermost layers and the underlying fiber layers were still intact suggesting surface degradation mechanism for PGS-PCL fibers. Scale bar 100 µm.
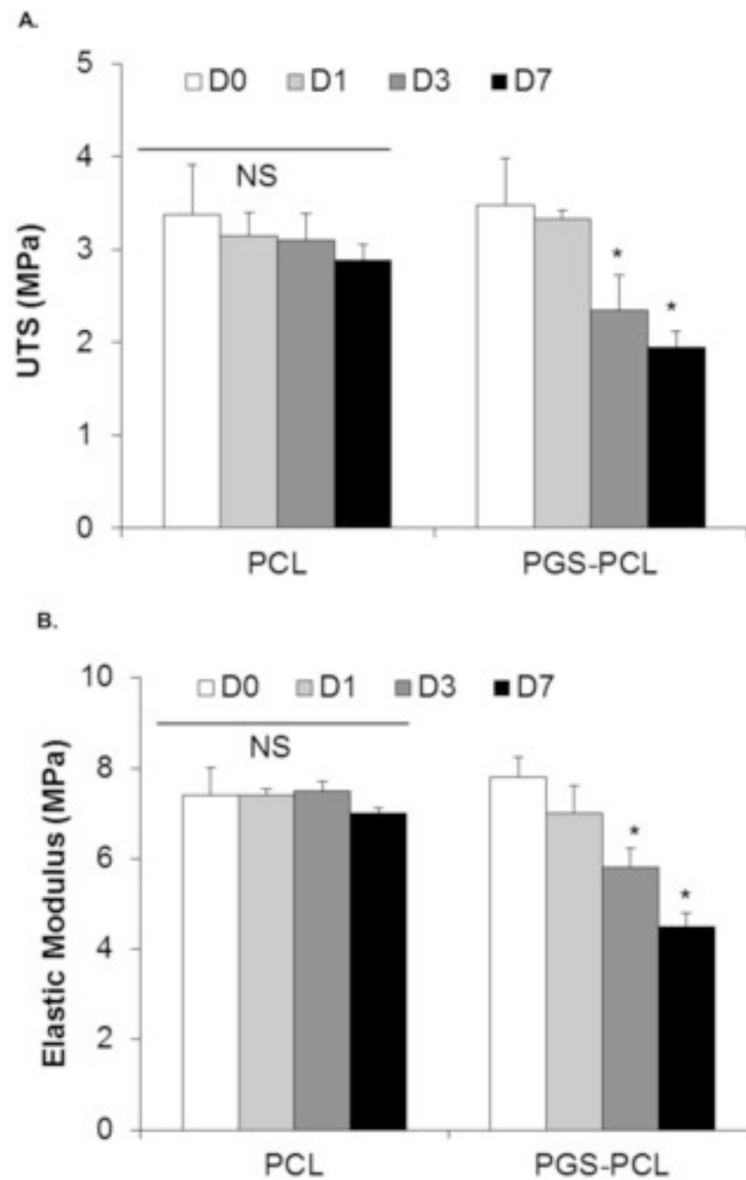
Fig. 3.
Effect of degradation on the mechanical properties of PCL and PGS-PCL scaffolds during accelerated degradation. The ultimate tensile strength (A) as well as Elastic moduli (B) of PCL scaffolds did not change significantly (One way ANOVA, p > 0.05; NS: non-significant) whereas those of PGS-PCL scaffolds showed significant decrease in the mechanical properties as an effect of degradation after day 1 (One way ANOVA, *p < 0.05).
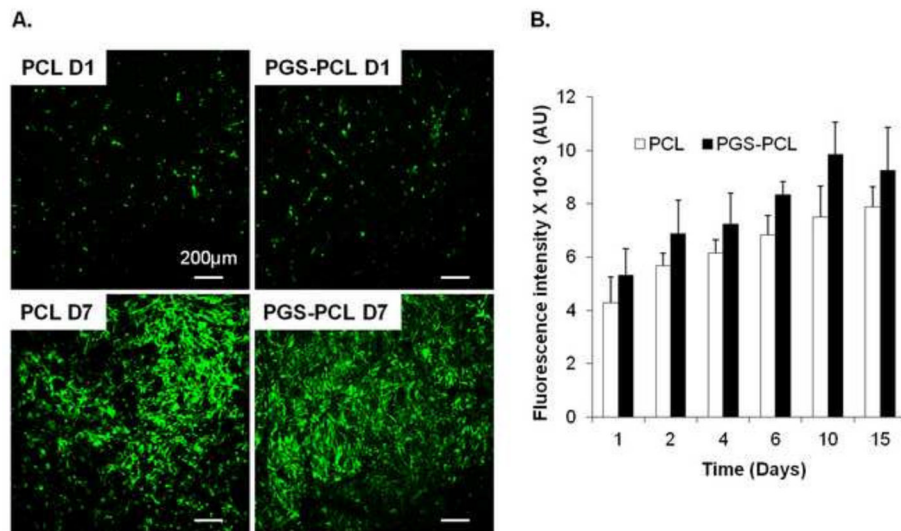
Fig. 4.
A. Viability of valve interstitial cells (VICs) on PCL and PGS-PCL scaffolds after 1 and 7 days in culture; B) Metabolic activity of VICs on PCL and PGS-PCL scaffolds over a period of 2 weeks. Cells were able to attach, spread and proliferate on both the scaffolds.
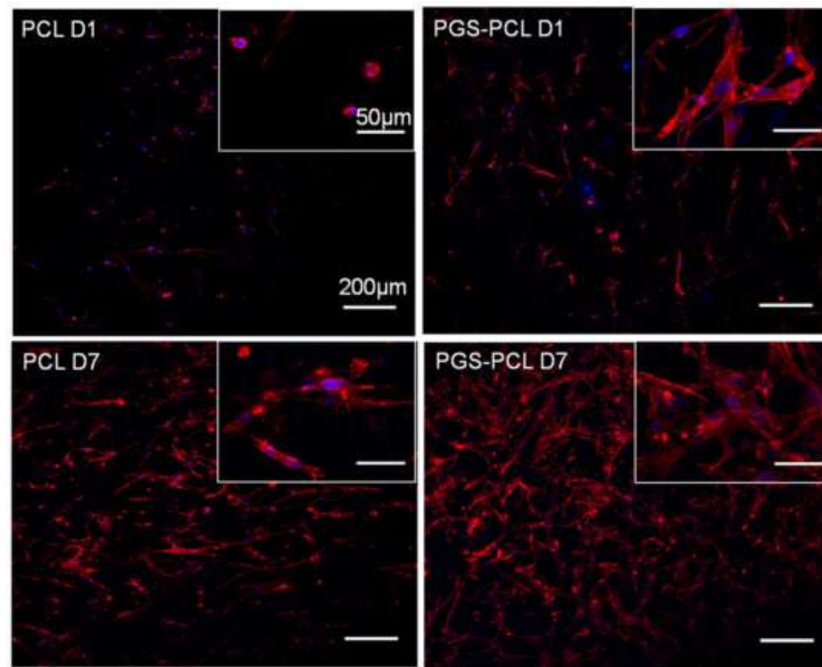
Fig. 5.
Morphology of MVICs on PCL and PGS-PCL scaffolds studied using actin-phalloidin staining. Cells showed rounded morphology on PCL whereas spread morphology on PGS-PCL as early as day 1. All the cells were spread by Day 7 on both the scaffolds.
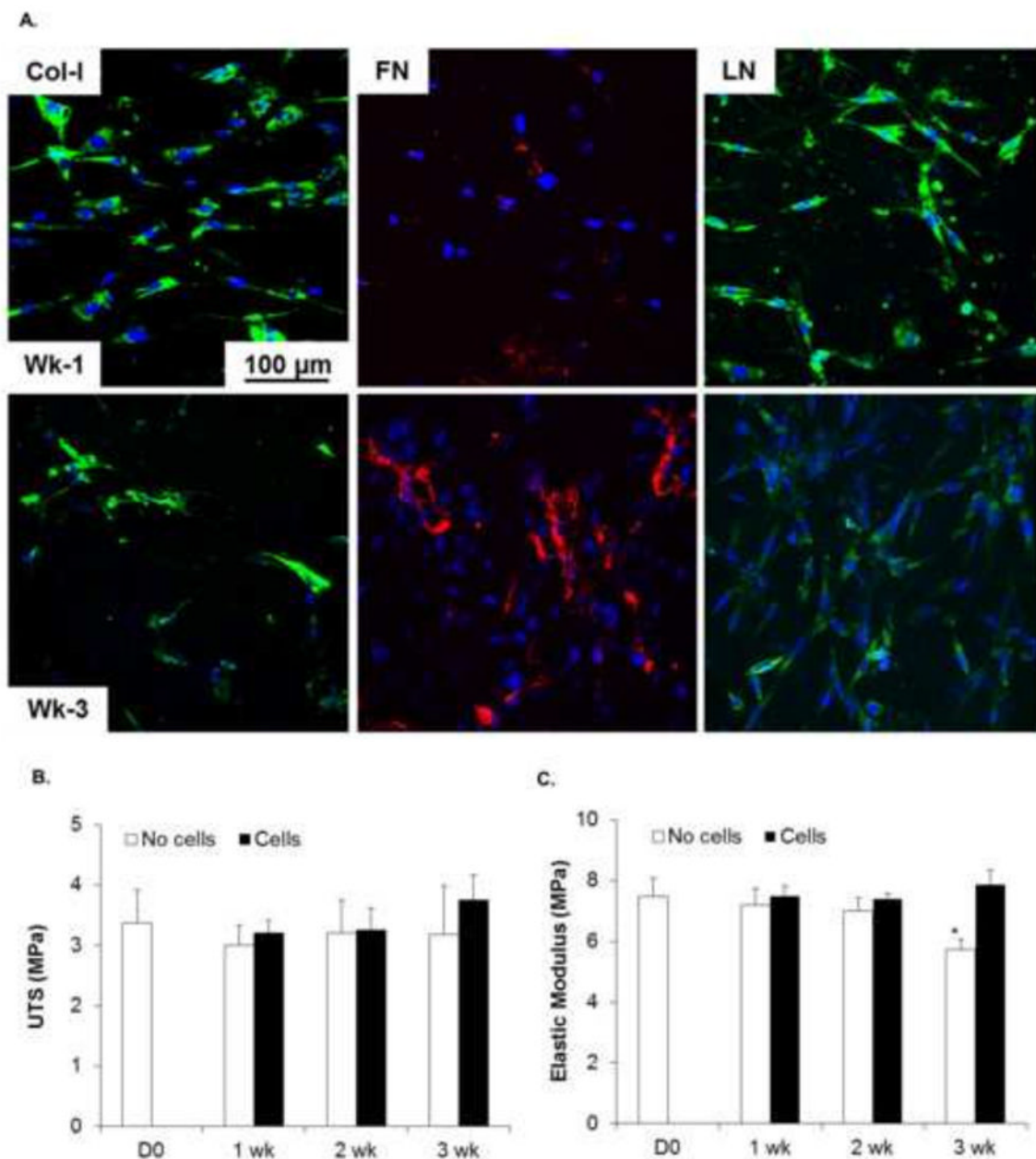
Fig. 6.
A. Evaluation of ECM secretion by VICs seeded on PCL scaffolds after 1 and 3 weeks in culture. Cell cultures were stained by immunostaining for collagen-I (Col-1), Fibronectin (FN) and Laminin (LN). PCL scaffolds showed less ECM production. B. Ultimate tensile stress (UTS) and C. Elastic moduli of PCL scaffolds. UTS of scaffolds without (empty bars) and with (filled bars) cells did not change significantly possibly due to slower rate of degradation and less amount of ECM secretion. ($p > 0.05$; Two way ANOVA followed by Post-hoc Fisher's LSD test). Significant reduction in Elastic moduli was observed for scaffolds cultured without cells only after 3 weeks compared to D0 and 1 week and compared to cell seeded scaffolds at 3 week (*$p < 0.05$, Two way ANOVA followed by Post-hoc Fisher's test).
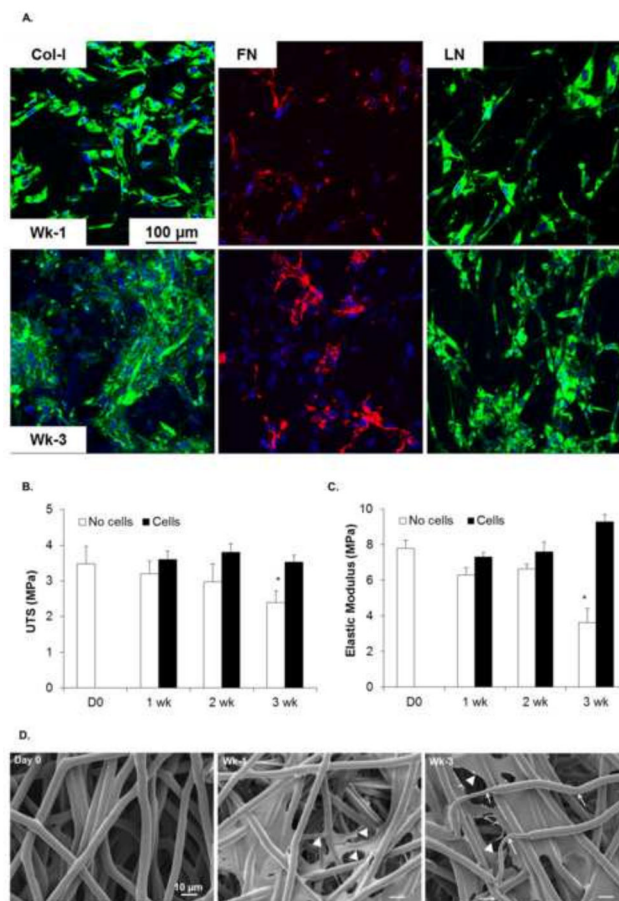
Fig. 7.
A. Evaluation of ECM secretion by VICs seeded on PGS-PCL scaffolds after 1 and 3 weeks in culture. Cell cultures were stained by immunostaining for collagen-I (Col-1), Fibronectin (FN) and Laminin (LN). PGS-PCL scaffolds showed enhanced ECM production compared to PCL scaffolds. B. UTS of PGS-PCL scaffolds without (empty bars) and with (filled bars) cells. PGS-PCL scaffolds without cells showed gradual decrease in UTS with significant decrease after 3 weeks (*P < 0.05, Two way ANOVA followed by Fisher's LSD test). The scaffolds seeded with the cells were able to maintain the mechanical properties due to balance between scaffold degradation and formation of new matrix. Two way ANOVA followed by Post-hoc Fisher's LSD test also revealed statistically significant differences between UTS of scaffolds with and without cells. C. Elastic moduli of PGS-PCL scaffolds; Significant changes in Elastic moduli was observed for scaffolds cultured without cells for all the time points except for 1week compared to 2 and 3 week culture (*p < 0.05). Two way ANOVA followed by Post-hoc Fisher's test also revealed significant differences in Elastic moduli of the scaffolds cultured with and without cells, suggesting the ability of the cells to remodel the synthetic scaffolds. D. Scanning electron microscopy images of PGS-PCL scaffolds at Day 0 and after 1 week and 3 week cell culture. Cells are marked with triangular arrowheads. White arrows indicate thinning of he fibers after 3 week culture.

Table 1

Summary of thermal properties of PCL scaffolds

Sample–	$T_{\text{m-PCL}}$- (°C)-	$T_{\text{c-PCL}}$- (°C)-	$\Delta\text{-}H_{\text{m-PCL}}$- (J/g)-
PCL polymer–	57.8-	25.29-	47.96-
PCL-D0–	56.1-	28.61-	26.35-
PCL-D3–	57.1-	28.79-	25.27-
PCL-D7–	57.0-	28.53-	25.18-

Table 2

Summary of thermal properties of PGS-PCL scaffolds

Sample–	$T_{\text{m-PGS}}$ (°C)-	$T_{\text{c-PGS}}$- (°C)-	Δ-$H_{\text{m-PGS}}$- (J/g)-	$T_{\text{m-PCL}}$- (°C)-	$T_{\text{c-PCL}}$- (°C)-	$\Delta H_{\text{m-PCL}}$- (J/g)-
PGS polymer–	15.0-	−10.15-	19.13-	--	--	--
PGS-PCL-D0–	12.2-	−11.4- −3.55-	2.58-	55.8-	29.51-	20.78-
PGS-PCL-D3–	12.6-	3.8- 15.53- −5.0-	0.8-	56.9-	29.12-	18.06-
PGS-PCL-D7–	12.6-	3.9- 18.01-	0.8-	56.6-	28.7-	18.08-